A-face-centered $Bi_{0.75}Ca_{3.25}Mn_3O_{10}$: A Bi-based orthorhombic 4310-type bilayered manganite

Y. L. Qin,[1] J. L. García-Muñoz,[2] H. W. Zandbergen,[1] and M. T. Casais[3]
[1]*National Center for HREM, Laboratory of Materials Science, Delft University of Technology, Rotterdamseweg 137, 2628 AL Delft, The Netherlands*
[2]*Institut de Ciència de Materials de Barcelona, CSIC, Campus Universitari de Bellaterra. E-08193, Bellaterra, Spain*
[3]*Instituto de Ciencia de Materiales de Madrid, C.S.I.C., Cantoblanco, E-28049 Madrid, Spain*
(Received 6 February 2001; published 4 October 2001)

We present electron diffraction and high-resolution electron microscopy measurements characterizing the structure of a Bi-based layered manganite. The crystal structure of $Bi_{0.75}Ca_{3.25}Mn_3O_{10}$ is orthorhombic and *A* centered (space group $A2_122$), with lattice parameters $a \cong b = 0.55$ nm and $c = 2.78$ nm. High-resolution electron microscopy reveals a well-defined 4310-type layered structure, identified as a member of the Bi-based Ruddlesden-Popper series with $n = 3$.

DOI: 10.1103/PhysRevB.64.172405 PACS number(s): 71.45.Lr, 71.38.−k, 71.27.+a, 68.37.Lp

I. INTRODUCTION

Manganese oxides have stimulated considerable scientific and technological interest because they present the colossal magnetoresistance (CMR) effect, whereby the magnetic field induces huge changes in the electrical conductivity.[1–3] Moreover, they exhibit other fascinating physical properties due to strong correlation effects between phononic, magnetic, and electronic degrees of freedom.[4] With the chemical composition $L_{1-x}A_xMnO_3$ (where *L* is a trivalent cation, usually a lanthanide, and *A* is a divalent cation), the mixed-valence state of Mn is tuned by the substitutional parameter *x*. The crystalline structure of most of these compounds is orthorhombic with *Pnma* symmetry. A key structural feature is the tilt of the MnO_6 octahedra, which leads to an $a_p\sqrt{2}$, $2a_p$, $a_p\sqrt{2}$ enlarged unit cell, where a_p is the simple perovskite lattice parameter.[5,6] Beside the technologically important CMR effect, other effects (e.g., the tendency displayed by many manganites to present a real-space ordering of the occupied orbitals and charges) are the subject of a growing research effort. There is also a strong interest in the physical and structural properties of the related manganites. Exploring new crystal structures is one of the indispensable efforts in the search for an optimized magnetoresistive response.

Recently, intense research has focused on some members of the Ruddlesden-Popper (RP) structural type series $A_{n+1}B_nO_{3n+1}$, with $n \neq \infty$, in particular the layered perovskites $(La,A)_{n+1}Mn_nO_{3n+1}$ (A = Ca, Sr) with $n = 1$ and $n = 2$. The perovskite structure corresponds to the $n = \infty$ member of the RP structural type. $n = 1$ is the well-known K_2NiF_4 structure $[(La,A)_2MnO_4]$, and $n = 2$ is the $Sr_3Ti_2O_7$ structure.[7] The $n \neq \infty$ structures are based on alternating rocksalt-type block layers *AO* and BO_2 layers, according to $AO\text{-}(BO_2\text{-}AO)_n$. Here *n* corresponds to the number of layers of corner-sharing BO_6 octahedra, which form structural blocks along the *c* axis. Most of the layered perovskites $(La,A)_{n+1}Mn_nO_{3n+1}$ ($n = 1,2$) have a body-centered-tetragonal structure with $I4/mmm$ symmetry. Tunneling or spin valve-based devices have been proposed based on RP compounds such as $(La, Sr)_{n+1}Mn_nO_{3n+1}$, as they present a natural stacking of perovskite bilayers.[4,8] Furthermore, pronounced CMR has been recently found in $La_{2-2x}A_{1+2x}Mn_2O_7$ ($n = 2$) for $0.2 \leqslant x \leqslant 0.5$.[4,8,9] Enhanced low-field MR was initially reported in $La_{1.2}Sr_{1.8}Mn_2O_7$, which is related to the lowering of the metal-insulator transition temperature under field (concomitant with the onset of magnetic ordering).[4,8,9] Moritomo *et al.* reported a 20 000% MR ($T_C = 129$ K, $H = 7$ T) in $La_{1.2}Sr_{1.8}Mn_2O_7$.[4] Moreover, orbital and charge-ordered phases have been identified in $(La, Sr)_2MnO_4$ ($n = 1$) (Refs. 10 and 11) and $LaSr_2Mn_2O_7$ ($n = 2$) materials.[12,13]

Given the interesting properties of La manganites, we recall that Bi^{3+} and La^{3+} ions have a very similar ionic size in many isostructural compounds,[14] which have almost identical unit cell volumes. However, the highly polarizable $6s^2$ lone pair of Bi^{3+} gives rise to clearly distinct physical features in many other cases. In Bi-based manganites the electronic configuration of Bi^{3+} seems to play an important role. As an example, $LaMnO_3$ is an orthorhombic (Pnma) antiferromagnet, while $BiMnO_3$ is monoclinic ($C2$) and ferromagnetic below $T_c = 100$ K.[15] Doping with Ca, $Bi_{2/3}Ca_{1/3}MnO_3$ is antiferromagnetic and insulating at low temperature, while $La_{2/3}Ca_{1/3}MnO_3$ is ferromagnetic and metallic.[16]

During a systematic study of the $(BiCa)MnO_3$ family, in particular, the $Bi_{1/4}Ca_{3/4}MnO_3$ compound,[16] a new layered manganite has been identified. The new orthorhombic phase has $a \cong b = 0.55$ nm and $c = 2.78$ nm and is *A* centered. It is the first time that a Bi-based (Bi-Ca-Mn-O) member of the RP structural type series with $n = 3$ has been identified. Using electron diffraction and high-resolution electron microscopy (HREM), we have characterized the structural features of this Bi-4-3-10 layered manganite.

II. EXPERIMENT

A black polycrystalline sample was synthesized under oxygen pressure from high-purity powders of Bi_2O_3, $CaCO_3$ and Mn_2O_3, mixed in the proportion corresponding to Bi(0.25)-Ca(0.75)-Mn-O(3). Prior to use, the powders were dehydrated at 900 °C for 12 h. The stoichiometric mixture was thoroughly ground in an agate mortar and pressed into a pellet. After sintering in an alumina crucible at various temperatures increased from 900 to 1050 °C with intermediate

 ©2001 The American Physical Society

grindings, the sample was pressed into a pellet and finally annealed at 1100 °C under 200 bars oxygen pressure for 24 h. The sample was then cooled to room temperature at a rate of 300 °C per hour. Thin specimens for electron microscopy were prepared simply by crushing the sample with an agate mortar and pestle. Crushed fragments were mixed with ethanol and then deposited onto a Cu grid coated with a thin carbon film. Electron microscopy was performed with a Philips CM30T and a Philips CM30UT-FEG electron microscope, both operating at 300 kV and with a Link EDX detector. Three different phases were observed at room temperature: the main nominal phase $Bi_{0.25}Ca_{0.75}MnO_3$ (with Pnma symmetry and an $\sqrt{2}a_p$, $2a_p$, $\sqrt{2}a_p$ enlarged unit cell), some grains containing the 327-type phase reported in Ref. 17, and finally the orthorhombic $(Bi, Ca)_4Mn_3O_{10}$ phase. The composition determination of the new orthorhombic Bi-Ca-Mn-O phase was performed by quantitative EDX using a spot size of about 20 nm in the Philips CM30UT electron microscope. Quantitative analysis performed in several microcrystallites indicated a composition $(Bi, Ca)_4Mn_3O_{10}$ with a Bi/Ca ratio ≈ 0.23. Thereby the stoichiometry is close to $Bi_{0.75}Ca_{3.25}Mn_3O_{10}$. In the notation $Bi_{3-3x}Ca_{1+3x}Mn_3O_{10}$, the parameter x $(=0.75)$ represents the concentration of Mn^{4+} ions (holes) in the bilayers.

III. RESULTS

A. Electron diffraction patterns

Two different types of symmetry are observed in the currently studied $Bi_{0.75}Ca_{3.25}Mn_3O_{10}$ compound: (i) *A*-centered orthorhombic and (ii) primitive orthorhombic.

1. A-Centered symmetry

At room temperature, the electron diffraction patterns (EDP's) on the $Bi_{0.75}Ca_{3.25}Mn_3O_{10}$ crystalline phase prove this phase to have orthorhombic symmetry. The [010], [−130], [−120], and [−110] EDP's are shown in Figs. 1(a), 1(b), 1(c), and 1(d), respectively. All these selected-area EDP's of $Bi_{0.75}Ca_{3.25}Mn_3O_{10}$ were obtained by tilting the specimen about the [001]* direction. From the diffraction spots along the reciprocal axis a^* in Fig. 1(a), the lattice parameters of the $Bi_{0.75}Ca_{3.25}Mn_3O_{10}$ phase are $a \cong b = 0.55$ nm (we recall that we do not appreciate different *a* and *b* lattice parameters because small orthorhombic distortions cannot be resolved from our measurements.) The lattice parameter of the long axis was determined from the *0014* spot in the 00*l* row along the c^* direction in Fig. 1(a), $c = 2.78$ nm. Indexation of all EDP's reveals an *A*-centered orthorhombic structure. The observed reflection conditions were the following: $k+l=2n$ for *hkl*, $l=2n$ for *h*0*l*, and $h=2n$ for *h*00. Consequently, these systematic absences with the use of the International Tables for Crystallography (1983) indicate that the possible extinction symbol of $Bi_{0.75}Ca_{3.25}Mn_3O_{10}$ is $A2_1$-*a*, *A*-*a*, or $A(bc)$-*a*. Further convergent-beam electron diffraction (CBED) experiments show that there is no mirror plane at all, which rule out other possibilities. Therefore, the possible space group is suggested to be $A2_122$.

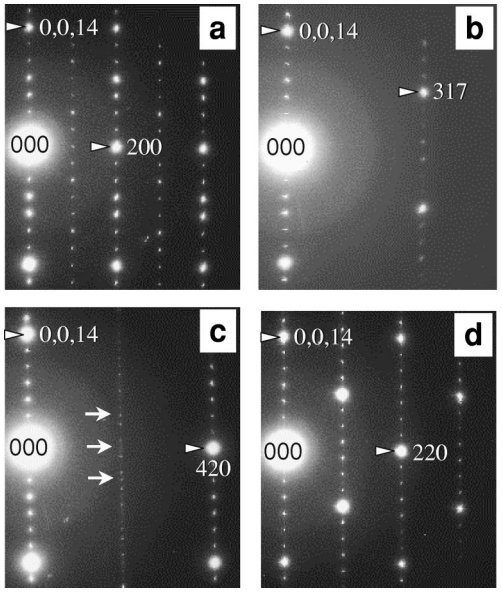

FIG. 1. Electron diffraction patterns from the $Bi_{0.75}Ca_{3.25}Mn_3O_{10}$ phase along (a) [010], (b) [−130], (c) [−120], and (d) [−110] zone axes.

In the EDP of Fig. 1(c), some additional spots are also visible (indicated by arrowheads), which can be indexed by assuming the presence of *a*-*b* twinned regions. As expected for this case, the diffraction patterns are a mixture of $A2_122$ and $B22_12$ symmetries.

2. Primitive orthorhombic symmetry

The absence of *A*-centered symmetry $(k+l \neq 2n)$ is frequently observed by the appearance of superreflections along the c^* direction, which can be seen clearly in Fig. 2. These $k+l \neq 2n$ reflections lead to a primitive orthorhombic symmetry. It is apparent that these reflections are much weaker in the [010] EDP [Fig. 2(a)] than those of the [−110] EDP [Fig.

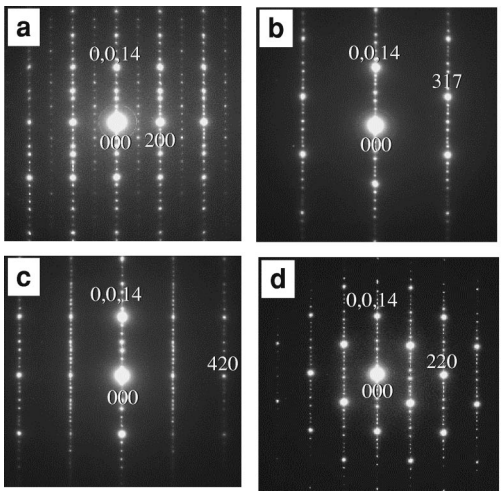

FIG. 2. Electron diffraction patterns from the $Bi_{0.75}Ca_{3.25}Mn_3O_{10}$ phase along (a) [010], (b) [−130], (c) [−120], and (d) [−110] zone axes, showing $k+l \neq 2n$ reflections along the c^* direction.

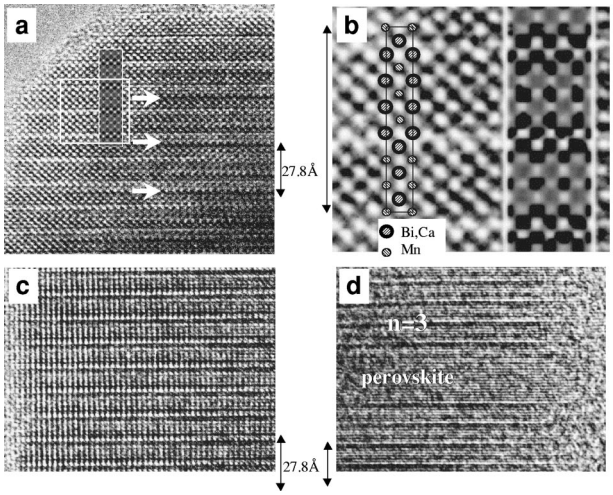

FIG. 3. HREM images projected along (a) $[-110]$ and (c) [010] zone axes. (b) A blowup outlined in (a), with the schematic crystal structure [based on the structural model of the layered manganites $(La, Sr)_{n+1}Mn_nO_{3n+1}$ phases, Refs. 10 and 14] projected along $[-110]$ direction superimposed on it. Only metal atoms are shown. (d) HREM image projected along the $[-120]$ zone axis, showing perovskite phase intergrowths in the $Bi_{0.75}Ca_{3.25}Mn_3O_{10}$ phase.

2(d)], and they even cannot be seen along $h=2n+1$ rows. It is not possible to determine its space group unambiguously from present data. However, it should be noted that $Ca_4Ti_3O_{10}$ adopts the *Pbca* symmetry,[18] and it is quite possible that the $Bi_{0.75}Ca_{3.25}Mn_3O_{10}$ phase can also adopt this symmetry next to the $A2_122$ symmetry described above. With the symmetry of *Pbca* (the reflection conditions are $k=2n$ for $0kl$ and $l=2n$ for $h0l$), Fig. 2(a) can be explained by a mixture of [100] and [010] axis EDP's. This would require that the crystal is *a-b* twinned, which is quite plausible since the *A*-centered structure also shows *a-b* twinning.

B. High-resolution electron microscopy

In order to confirm the layer-stacking mode of this new Bi-based manganite, we carried out an HREM study. The main results are shown in Figs. 3(a)–3(d). HREM images give evidence of large regions of the $Bi_{0.75}Ca_{3.25}Mn_3O_{10}$ phase, having well-defined $A_4Mn_3O_{10}$-type layered structure. Figure 3(a) and 3(c) are HREM images taken in a thin region of the crystal with the incident beam along $[-110]$ and [010] zone-axis directions, respectively. In these images, the rows of the brightest dots are related to (Bi, Ca)O layers sandwiched by MnO_2 layers. Figure 3(b) shows an enlarged part of Fig. 3(a), with an atomic model of the crystal structure superimposed onto it. The metal atom positions are imaged as dark dots. A calculated image [based on the structural model for the layered $(La, Sr)_{n+1}Mn_nO_{3n+1}$ phases given in Refs. 7 and 10], superimposed onto the images of Figs. 3(a) and 3(b), is in good agreement with the experimental one.

Intergrowths of the 113-perovskite phase have been also observed in the 4310-type crystals. Figure 3(d) shows an example of a 113-perovskite intergrowth in the $Bi_{0.75}Ca_{3.25}Mn_3O_{10}$ phase. In the right part of Fig. 3(a), one can also see some contrasts (indicated by arrows) which display the same periodicity as the *c* axis. They might be due to an ordering of Bi and Ca in the two (Bi, Ca)O planes, forming the rocksalt blocks, and can produce the superreflections shown in Fig. 2.

IV. DISCUSSION AND CONCLUSIONS

Ruddlesden and Popper[7] studied the series $Sr_{n+1}Ti_nO_{3n+1}$ ($n=1$, 2, and 3) and recognized their structures as higher-order polytypes of K_2NiF_4 structure type. The space group $I4/mmm$ was obtained from their x-ray powder diffraction photograph. In this SrO-TiO_2 series the TiO_6 octahedra have their fourfold axes aligned with the unit-cell edges. Lately, Elcombe *et al.*[18] investigated the structures of the RP phases $Ca_{n+1}Ti_nO_{3n+1}$. With the tilted TiO_6 octahedra, the $CaTiO_3$ ($n=\infty$) end member has the orthorhombic symmetry with space group *Pnma*. The structures of $Ca_3Ti_2O_7$ ($n=2$) and $Ca_4Ti_3O_{10}$ ($n=3$) were determined to be $A2_1am$ and *Pbca* by CBED experiments and neutron powder diffraction. They predicted that all $A_{n+1}B_nX_{3n+1}$ series for which the $n=\infty$ end member (ABX_3) is isostructural with $CaTiO_3$ would be isostructural with the compounds $Ca_{n+1}Ti_nO_{3n+1}$. If this is the case, the recently found layered manganites $(La\text{-}A)_3Mn_2O_7$ ($A=Sr, Ca$) and $(La, Ca)_4Mn_3O_{10}$ (Ref. 19) should have the symmetry of $A2_1am$ and *Pbca*, respectively, because $(La\text{-}A)MnO_3$ also has the *Pnma* structure. However, the body-centered-tetragonal structure for these compounds was obtained from x-ray diffraction data, but detailed determination was not given. More recently, the structure of $(Bi, Ca)_3Mn_2O_7$ has been investigated by CBED and HREM measurements.[17] At both low temperature and room temperature (RT), the crystal presents Amam symmetry.

There are two different types of symmetry in this $Bi_{0.75}Ca_{3.25}Mn_3O_{10}$ compound. The primitive orthorhombic structure is observed more often than *A*-centered phase. Figure 4 shows schematic structures of the Mn-based layered perovskite $(Bi, Ca)_{n+1}Mn_nO_{3n+1}$ with $n=2$ (a) and $n=3$ (b), (c). The two types of symmetry differ in the way that neighboring perovskite blocks are coupled. In the *A*-centered phase the MnO_6 octahedra of neighboring perovskite blocks are tilted in the same way [see Figs. 4(a) and 4(b)]. On the other hand, if they tilt in a different way, then a primitive-orthorhombic structure is obtained [Fig. 4(c)]. Obviously, the coupling between these perovskite blocks is governed by the distortions in the rocksalt like layers (*A*O layers) between the perovskite blocks. For the $n=2$ phase the oxygen atoms and the large cations in the neighboring *A*O layers shift in the same direction [see arrows in Fig. 4(a)], resulting in an *A*-centered structure.[17] Based on the $n-2$ structure, one would expect that the oxygen atoms and the large cations in

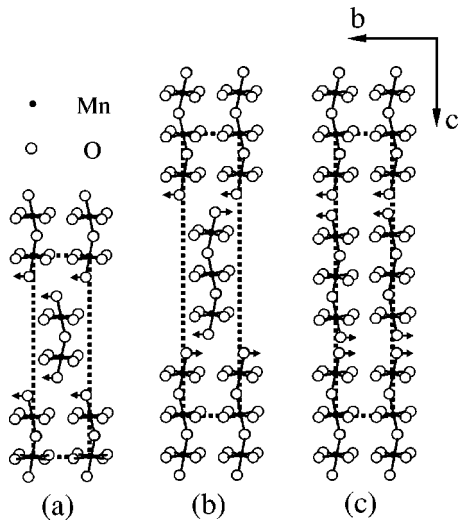

FIG. 4. Schematic structures of the Mn-based layered perovskite $(Bi, Ca)_{n+1}Mn_nO_{3n+1}$ with $n=2$ (a) and $n=3$ (b), (c). Only the MnO_6 octahedra are shown in polyhedral representations. The unit cells are outlined by dashed lines. The shifts in neighboring rocksalt planes is indicated with arrows.

the neighboring AO layers shift also in the same direction, resulting in a primitive space group, which is indeed observed the most. However, the $n=3$ phase occurs also with *A*-centered structure, indicating that the coupling of the octahedra tilts of neighboring perovskite blocks through the shifts in the AO layers is not very strong. This is also in agreement with the observation of frequent *a-b* twinning.

Finally, we want to emphasize the outstanding role that the Bi^{3+} lone pair plays in some families of $n=\infty$ manganites:[15,16,20–22] to be recalled here is the spectacularly high orbital and charge ordering temperature, $T_{CO}=525$ K, recently found in $Bi_{1/2}Sr_{1/2}MnO_3$.[20] Due to the dominant character of the $6s^2$ lone pair in this Bi-based manganite, the charges order approximately 450 K above the temperature predicted by the bandwidth tuning mechanism for the $L_{1/2}(Ca; Sr)_{1/2}MnO_3$ family[20–22] ($L \neq Bi$). On another hand, less spectacular, but without a clear explanation yet, $Bi_{1/2}Ca_{1/2}MnO_3$ is the only half-doped $n=\infty$ manganite with $T_{CO}>300$ K (RT) ($T_{CO}=325$ K). These are apparent examples of the importance of exploring new Bi-based manganese oxides.

To summarize, we have reported observation of a 4310-type layered structure in the Bi-Ca-Mn-O phase diagram [$n=3$ member of the Ruddlesden-Popper $(Bi, Ca)_{n+1}Mn_nO_{3n+1}$ series]. According to the different physical properties of the $n=\infty$ La and Bi manganites,[15,16,20–22] also a very different physical behavior is expected in Bi-based layered $(Bi, Ca)_4Mn_3O_{10}$ oxides respect to $(La, Ca)_4Mn_3O_{10}$ compounds. The crystal structures of the $Bi_{0.75}Ca_{3.25}Mn_3O_{10}$ phase, obtained under high oxygen pressure, have been investigated by transmission electron microscopy and HREM measurements. At room temperature two different types of symmetry are observed in the present $Bi_{0.75}Ca_{3.25}Mn_3O_{10}$ compound: primitive orthorhombic and *A* centered with space group $A2_122$. From the different couplings of the octahedra tilts of neighboring perovskite blocks described in these two phases, a more pronounced two-dimensional behavior is expected in the *A*-centered phase.

ACKNOWLEDGMENTS

The authors acknowledge financial support by Stichting voor Fundamenteel Onderzoek der Materie (FOM), CICyT (MAT97-0699), MEC (PB97-1175), Generalitat de Catalunya (GRQ95-8029), INTAS (Project No. 971-11954), and the EC through the ''Oxide Spin Electronics'' (OXSEN) network (TMR).

[1] R. von Helmolt *et al.*, Phys. Rev. Lett. **71**, 2331 (1993).
[2] S. Jin *et al.*, Science **264**, 413 (1994).
[3] C. N. R. Rao and A. K. Cheetham, Science **272**, 369 (1996).
[4] Y. Moritomo *et al.*, Nature (London) **380**, 141 (1996).
[5] P. G. Radaelli *et al.*, Phys. Rev. Lett. **75**, 4488 (1995).
[6] J. L. García-Muñoz *et al.*, Phys. Rev. B **55**, 34 (1997).
[7] S. N. Ruddlesden and P. Popper, Acta Crystallogr. **54**, 11 (1958).
[8] T. Kimura *et al.*, Science **274**, 1698 (1996).
[9] H. Asano, J. Hayakawa, and M. Matsui, Phys. Rev. B **68**, 5395 (1997).
[10] R. H. Heffner *et al.*, Phys. Rev. Lett. **81**, 1706 (1998).
[11] Y. Moritomo *et al.*, Phys. Rev. B **51**, 3297 (1995).
[12] W. Bao *et al.*, Solid State Commun. **98**, 55 (1996).
[13] T. Kimura *et al.*, Phys. Rev. B **58**, 11 081 (1998).
[14] R. D. Shannon, Acta Crystallogr., Sect. A: Cryst. Phys., Diffr., Theor. Gen. Crystallogr. **32**, 751 (1976).
[15] T. Atou *et al.*, J. Solid State Chem. **145**, 639 (1999).
[16] J. L. García-Munoz *et al.* (unpublished).
[17] Y. L. Qin *et al.*, Phys. Rev. B **63**, 144108 (2001).
[18] M. M. Elcombe *et al.*, Acta Crystallogr., Sect. B: Struct. Sci. **47**, 305 (1991).
[19] H. Asano, J. Hayakawa, and M. Matsui, Appl. Phys. Lett. **71**, 844 (1997).
[20] J. L. García-Muñoz *et al.*, Phys. Rev. B **63**, 064415 (2001).
[21] C. Frontera *et al.*, J. Phys.: Condens. Matter **13**, 1071 (2001).
[22] C. Frontera *et al.*, Phys. Rev. B **64**, 054401 (2001).